First-principles study on anatase TiO_2 (101) surface adsorption of NO*

Feng Qing(冯 庆)[a)b)†], Yue Yuan-Xia(岳远霞)[a)b)], Wang Wei-Hua(王渭华)[a)b)], and Zhu Hong-Qiang(朱洪强)[a)b)]

[a)] College of Physics and Electronic Engineering, Chongqing Normal University, Chongqing 401331, China
[b)] Chongqing Key Laboratory on Optoelectronic Functional Materials, Chongqing 401331, China

(Received 3 July 2013; revised manuscript received 26 August 2013; published online 20 February 2014)

In this paper, the stable structure and the electronic and optical properties of nitric oxide (NO) adsorption on the anatase TiO_2 (101) surface are studied using the plane-wave ultrasoft pseudopotential method, which is based on the density functional theory. NO adsorption on the surface is weak when the outermost layer terminates on twofold coordinated oxygen atoms, but it is remarkably enhanced on the surface containing O vacancy defects. The higher the concentration of oxygen vacancy defects, the stronger the adsorption is. The adsorption energies are 3.4528 eV (N end adsorption), 2.6770 eV (O end adsorption), and 4.1437 eV (horizontal adsorption). The adsorption process is exothermic, resulting in a more stable adsorption structure. Furthermore, O vacancy defects on the TiO_2 (101) surface significantly contribute to the absorption of visible light in a relatively low-energy region. A new absorption peak in the low-energy region, corresponding to an energy of 0.9 eV, is observed. However, the TiO_2 (101) surface structure exhibits weak absorption in the low-energy region of visible light after NO adsorption.

Keywords: anatase TiO_2 (101) surface, first-principles, density functional theory, electronic structures

PACS: 31.15.A–, 71.15.Dx, 71.15.Mb, 71.15.–m **DOI:** 10.1088/1674-1056/23/4/043101

1. Introduction

Motor vehicle exhaust gas mainly consists of NO and NO_2, among others. Researchers have found that light catalytic oxidation technology can effectively remove pollutants. Wang,[1] Wang and Meng,[2] and Wang and Liu[3] used different computational methods to study the adsorption and desorption of NO gas on rutile TiO_2 (110). Their calculations showed that NO on the TiO_2 surface is adsorbed via bridge chemical adsorption. Ma *et al.*[4] and Ma[5] conducted a fundamental research on anatase TiO_2 (101) surface modification using sulphur (S). Based on the adsorption energy calculations, S may be adsorbed at a Ti vacancy, and S adsorption on the anatase TiO_2 (101) surface is more stable than on the rutile TiO_2 (110) surface.

Chen *et al.*[6] and Chen and Tang[7] conducted a nitrogen/fluorine (N/F) doping to characterise the anatase TiO_2 (101) surface. They found that the adsorption of N atoms forms two shallow occupied levels, which improve the TiO_2 photocatalytic ability, whereas the adsorption of F atoms does not improve the adsorption performance of TiO_2. Sun and Shi[8] built a photocatalytic test cabin and repeatedly measured the NO_x purification efficiency by loading white concrete pavement materials, under different lights, temperature, and water scour conditions. The results show that under the ideal conditions of 4% TiO_2 material pavement load and 6-h adsorption, the NO removal efficiency reaches 95%, and NO_2 purification efficiency reaches nearly 90%. For a 10-h adsorption, the NO_x purification efficiency is close to 100%. In recent years, experimental research and theoretical calculations have mostly concentrated on surface adsorption.[9–12] Recently, there has been some research on the optical gas sensitive effect of metal–oxide material, namely, through the changes of optical properties (including absorptivity, reflectivity, etc.) to extract the gas content of the environment. Wanbayor and Ruangpornvisuti[13] have investigated the adsorptions of di-, tri-, and poly-atomic gases on the anatase TiO_2 (001) and (101) surfaces and their adsorption abilities. However, there have been few theoretical researches conducted on the electronic and optical properties of nitride adsorption on the anatase TiO_2 (101) surface. In this paper, we focus on the studies of the electronic and optical properties and stable structures of the anatase TiO_2 (101) surface after molecular NO adsorption using the first-principles density functional theory.

2. The model construction and computational method

According to our previous surface calculation results and those given by Ma *et al.*,[14] the most stable anatase TiO_2 (101) surface structure has an outermost layer that terminates in a two-coordinate O (O_{2c}), followed by a second layer with a five-coordinate Ti (Ti_{5c}) and a third layer with a three-coordinate O (O_{3c}). An O_{2c} position is selected for the shear position, and an 18-layer surface structure model, with upper and lower vacuum thickness values of 0.8-nm each, was es-

*Project supported by the National Natural Science Foundation of China (Grant Nos. 61106129 and 61274128).
†Corresponding author. E-mail: fengq_126@163.com
© 2014 Chinese Physical Society and IOP Publishing Ltd

tablished, 2×2 super-cell is built, and the conditions are optimized. The middle 12 layers of atoms are all aligned during geometry optimization. The surface structures before and after optimization are shown in Figs. 1(a) and 1(b), respectively. After optimization, the superficial atoms undergo relaxation, but no reconstruction phenomenon occurs. After the relaxation, the terminal atom of the outermost surface layer is still an O_{2c}. However, the sub-layer becomes an O_{3c}, and the third layer is converted into a Ti_{5c}. The 2×2 super-cell models act as adsorption substrates on which the NO molecules are built. The model is then placed in a cube and geometrically optimized. After optimization, the NO molecular bond length is determined to be 1.195 Å, and the system energy is −701.7850 eV. In this paper, the different ways of adsorbing NO molecule onto the TiO_2 (101) surface are discussed.

All computations are performed using the VASP software package.[15] All optimisation calculation methods are used in the GGA–PBESOL[16] to facilitate the comparison among the adsorption results. To ensure a balanced consideration of the computer calculation ability and calculation reliability, the energy convergence standard is set to be 2×10^{-5} eV/atom, the plane wave truncation is fixed at 300 eV, and the first Brillouin zone is set at a 4×3×1 division.

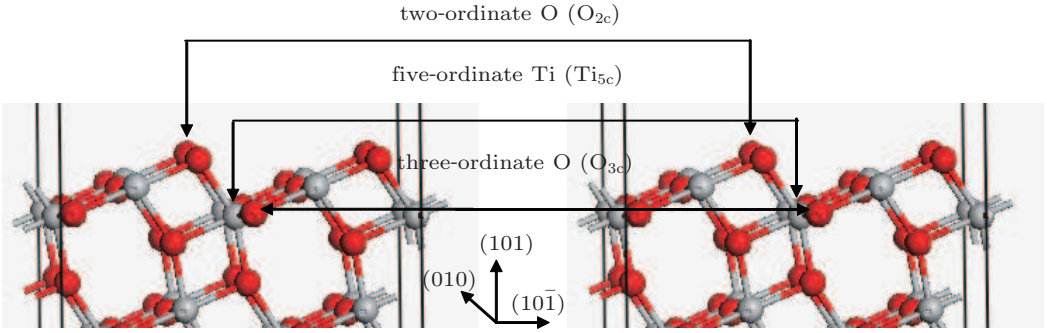


Fig. 1. (color online) Atomic structures of the anatase TiO_2 (101) surface before and after optimization.

3. Results and discussion

3.1. Formation of surface energy with O vacancy defects

The formation of surface energy with O vacancy defects and environment are closely related to each other. The anatase crystal surface structure, whose outermost and second layers are terminated by twofold coordinated oxygen atoms and fivefold coordinated titanium atoms, was found to be much more stable.[17] In the present paper, the O-rich environment and anoxic environment are considered. The formulas and calculation results are as follows:

$$E(\text{formation}) = E_{\text{T}}(\text{defect}) - E_{\text{T}}(\text{perfect}) + nu_{\text{O}}, \quad (1)$$

where $E_{\text{T}}(\text{defect})$ represents the total energy of the lattice system with O vacancy defects, $E_{\text{T}}(\text{perfect})$ is the total energy of the complete lattice system, u_{O} is the chemical potential of O, and n represents the number of O vacancies. The definition of an O-rich environment is

$$u_{\text{O}} = \frac{1}{2}u_{\text{O}_2}, \quad (2)$$

the definition of a hypoxic environment is

$$u_{\text{O}} = \frac{1}{2}(u_{\text{TiO}_2} - u_{\text{Ti}}), \quad (3)$$

with u_{Ti} representing the chemical potential of Ti, and u_{TiO_2} the chemical potential of TiO_2.

Table 1. Formation energy of surface O vacancy under an anoxic environment.

The concentration of O vacancy defects	0.25	0.5
The formation energy/eV	–6	–11.6

Table 2. Formation energy of surface O vacancy under an O-rich environment.

The concentration of O vacancy defects	0.25	0.5
The formation energy/eV	4.87	10.14

The results show that when the surface is in a hypoxic environment, it is easy to form an oxygen vacancy and the surface is stable. But it is difficult to form an oxygen vacancy in an O-rich environment.

3.2. Adsorption conditions

We choose the following four kinds of adsorption positions from which the calculated models are built:

(i) Vertical adsorption of NO with the N ending above the O_{2c} of the complete anatase TiO_2 (101) surface [Fig. 2(a)];

(ii) Vertical adsorption of NO with the N ending above the O_{3c} position [Fig. 2(b)];

(iii) Vertical adsorption of NO with the N ending above the Ti_{5c} position [Fig. 2(c)];

(Based on the results given by Wang and Liu[3] on the surface adsorption of NO molecules on rutile TiO_2 (110), the N atom of NO is easy to adsorb onto the Ti position)

(iv) Selection of the level of NO adsorption on the anatase TiO_2 (101) surface [Fig. 2(d)]. The corresponding structures after optimization are shown in Figs. 2(a′)–2(d′).

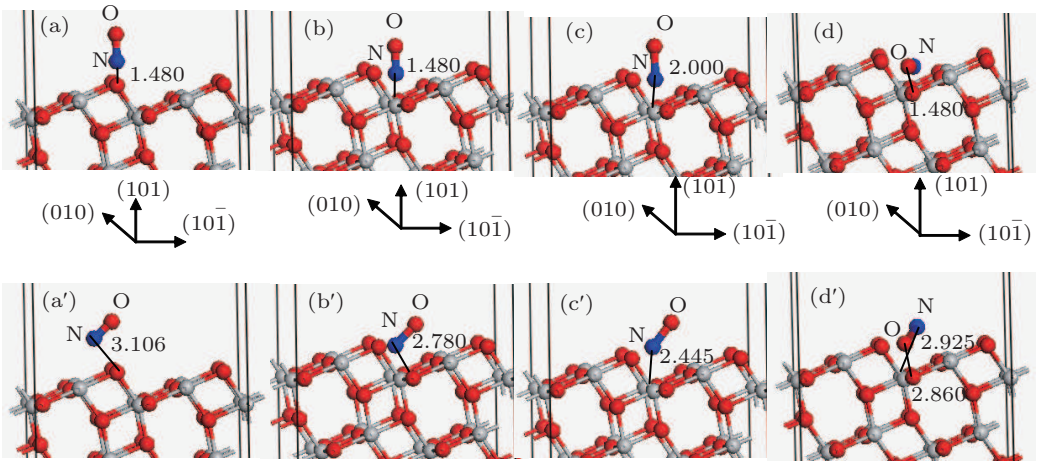


Fig. 2. (color online) Atomic structures of anatase TiO_2 (101) integrate surface before and after adsorption of NO.

Comparisons between Figs. 2(a) and 2(a′), 2(b) and 2(b′), and 2(c) and 2(c′) reveal that the N–O_{2c} bond length changes from 1.480 Å to 3.106 Å , the N–O_{3c} bond length increases from 1.480 Å to 2.78 Å, and the N–Ti_{5c} bond length changes from 2.000 Å to 2.445 Å. These three cases reveal that NO molecules with the three vertical adsorptions after the optimizations at different levels occur away from the substrate, thereby indicating weak adsorption on the surface. A comparison between Figs. 2(d) and 2(d′) shows that the N–O_{3c} bond length changes from 1.480 Å to 2.860 Å and that the NO molecules generally stay at a horizontal position of the surface after optimization. However, distances between the molecules and surface increase, further confirming the weak adsorption on the surface. The NO molecules in the complete O_{2c} surface are weakly adsorbed regardless of the adsorption method adopted. The interaction between the N atom of the NO molecules and the Ti surface is stronger in some parts.

The surface of the O_{2c} position at the terminal of the anatase TiO_2 (101) surface layer is loosely bonded to the Ti ion, thereby facilitating the formation of O vacancy defects. This observation also confirms the experimental results of Hebenstreit *et al.*[18] We also attempt to study the adsorption of NO molecules on the anatase TiO_2 (101) surface containing O vacancy defects.

Model building is conducted as follows: a surface two-coordinate O atom is removed from the two-coordinate O surface (Fig. 1(a)). The O vacancy concentration is set as 0.25, and geometry optimization is then performed. After optimization, the Ti atoms around the vacancy move outwards. These findings are consistent with those found in Ref. [19]. First, the N end of the NO molecule is vertically adsorbed on the TiO_2 (101) surface at the O vacancy portion [Fig. 3(a)]. The O end of the NO molecule is then vertically adsorbed on the O vacancy of the TiO_2 (101) surface [Fig. 3(b)]. For geometric optimization, the optimized structures of the corresponding absorption sites are shown in Figs. 3(a′) and 3(b′).

The N end of NO during adsorption on the surface at the O vacancy undergoes the following changes: the N–O_{3c} bond length changes from 2.960 Å to 2.626 Å, the N–Ti_{6c} bond length decreases from 3.030 Å to 2.063 Å, and the N–Ti_{5c} bond length is reduced from 2.295 Å to 1.896 Å [Figs. 3(a) and 3(a′)]. A comparison between Figs. 3(b) and 3(b′) shows that the O of NO at the O vacancy undergoes the following changes during adsorption: the O–O_{3c} bond length changes from 2.960 Å to 2.631 Å, the O–Ti_{6c} bond length decreases from 3.030 Å to 2.069 Å, and the O–Ti_{5c} bond length is reduced from 2.295 Å to 1.935 Å. These findings support the conclusion that NO is more easily adsorbed onto the surface containing O vacancy defects, regardless of the adsorption method. The N or O end of the NO molecules is substantially adsorbed on the surface at the O vacancy site.

The optimized model is used to determine the effects of the O vacancy concentration on NO adsorption on the anatase TiO_2 (101) surface. The two O_{2c} atoms of the surface are both removed, resulting in an O vacancy concentration of 0.5, the structure is shown in Fig. 3(c). Geometry optimization is then performed, and the optimization structure [Fig. 3(c′)] shows that the bond length of N–O_{3c} changes from the initial 3.493 Å to 2.565 Å, and that of O–O_{3c} decreases from 2.960 Å to 2.576 Å. In general, the bond lengths become shorter. As

observed from a local amplified vertical view, the bond length of N–Ti_{5c} decreases from 2.994 Å to 1.948 Å, that of N–Ti_{6c} decreases from 3.434 Å to 2.013 Å, that of O–Ti_{5c} is reduced from 2.319 Å to 2.069 Å, and that of O–Ti_{6c} changes from 2.857 Å to 2.281 Å. The N or O end, as well as the distance between surrounding Ti atoms, is significantly reduced, and NO is more easily adsorbed on the anatase TiO_2 (101) surface containing a high concentration of O vacancy defects. Therefore, a high concentration of O vacancy defects on the surface improves the NO adsorption.

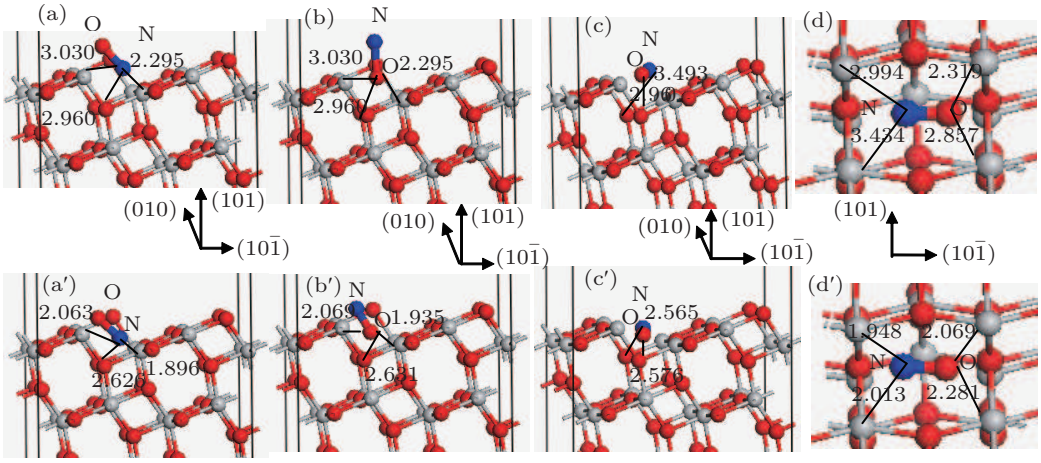


Fig. 3. (color online) Atomic structures of the anatase TiO_2 (101) surface with oxygen vacancies before and after adsorption of NO.

The aforementioned results show that a complete O_{2c} surface inhibits the adsorption of NO molecules, whereas the anatase TiO_2 (101) surface containing O vacancy defects promotes the adsorption.

3.3. Adsorption energy

In Ref. [20] the adsorption energy of the NO molecules on the TiO_2 (101) surface is defined as follows:

$$E_{\text{ads}} = (E_{\text{substrate}} + E_{\text{NO}}) - E_{(\text{NO+substrate})},$$

where E_{ads} is the surface adsorption energy, $E_{\text{substrate}}$ represents the total energy of the cell surface with O vacancies, E_{NO} is the NO molecular energy before adsorption, and $E_{(\text{NO+substrate})}$ is the total energy of the entire surface after absorption.

Table 3 shows that when the O vacancy concentration on the TiO_2 (101) surface is 0.25, the N end of the NO molecule is vertically adsorbed onto the surface, the calculated adsorption energy is 3.4528 eV, and the corresponding adsorption energy of the O vertical adsorption is 2.6770 eV. When the O vacancy concentration on the TiO_2 (101) surface is 0.5, the NO molecule level adsorbed on the surface has a corresponding adsorption energy of 4.1437 eV. The adsorption energy is positive, indicating an exothermic adsorption process. The adsorption energy of the NO horizontal adsorption on the surface is highest, indicating that surface adsorption is easiest. In addition, the surface with highly concentrated O vacancy defects promotes NO adsorption, and the adsorption structure tends to be more stable.

Table 4 shows the three adsorption methods for NO as well as the Mulliken charge densities of the N and O atoms. The charges of the N and O atoms in the three methods are different, and the O atomic charge value exhibits a larger difference. This finding explains the higher ability for an O atom to attract electrons, as well as its higher negative electric charge. After adsorption, the net charge of NO is negative, indicating that the electron is transferred from the Ti atom substrate to the NO molecule. When NO horizontal adsorption occurs on the surface, more charges transfer to the NO molecule, confirming that the adsorption bond is stronger and the adsorption condition is more stable. Therefore, the bond length of NO after the horizontal adsorption on the surface is longer than those of the other two methods, and the bond length after adsorption is 1.436 Å. This phenomenon also causes the N–O bond to weaken. The charge population after adsorption shows a strong interaction between the NO molecules and the substrate surface, indicating that NO is prone to adsorb onto the anatase TiO_2 surface containing O vacancy defects.

Table 3. Values of adsorption energy (eV) of NO on the TiO_2 (101) surface.

Adsorption form	E_{NO}/eV	$E_{\text{substrate}}$/eV	$E_{(\text{NO+substrate})}$/eV	E_{ads}/eV
N end adsorption	–701.7850	–29276.2992	–29981.5370	3.45
O end adsorption	–701.7850	–29276.2992	–29980.7612	2.68
NO horizontal adsorption	–701.7850	–28838.4489	–29544.3776	4.14

Table 4. Charge populations and the N–O bond lengths in the NO molecule.

	q_N (charge/e)	q_O (charge/e)	q_{NO} (charge/e)	N–O length/Å
Ideal NO molecule	0.13	–0.13	0.00	1.480
N end adsorption	–0.28	–0.24	–0.52	1.266
O end adsorption	–0.17	–0.38	–0.55	1.314
NO level adsorption	–0.41	–0.45	–0.86	1.436

3.4. Surface band structure and density of states

The band structures of the NO molecule before and after adsorption on the anatase TiO_2 (101) surface with one O vacancy are shown in Fig. 4.

For the electronic structure of the surface with O vacancies [Fig. 4(a)], the band gap is 2.6 eV; moreover, four new bands appear at the bottom of the conduction band (up arrow). The Fermi energy level passes through a new band. Thus, the electron absorbs a smaller amount of energy as the transition occurs, suggesting that the surface containing O vacancies has an absorption peak in the low-energy region.

The NO horizontal adsorption surface band structure [Fig. 4(b)] has a band gap width of 2.6 eV. The conduction band structure is similar to that of the O vacancy surface, and new bands are also observed (up arrow). The Fermi level also goes through a new band. Thus, the electrons absorb a smaller amount of energy, indicating that the absorption peaks would be found in the low-energy area of the adsorption surface. The figures also show two new bands in the band gaps (down arrows).

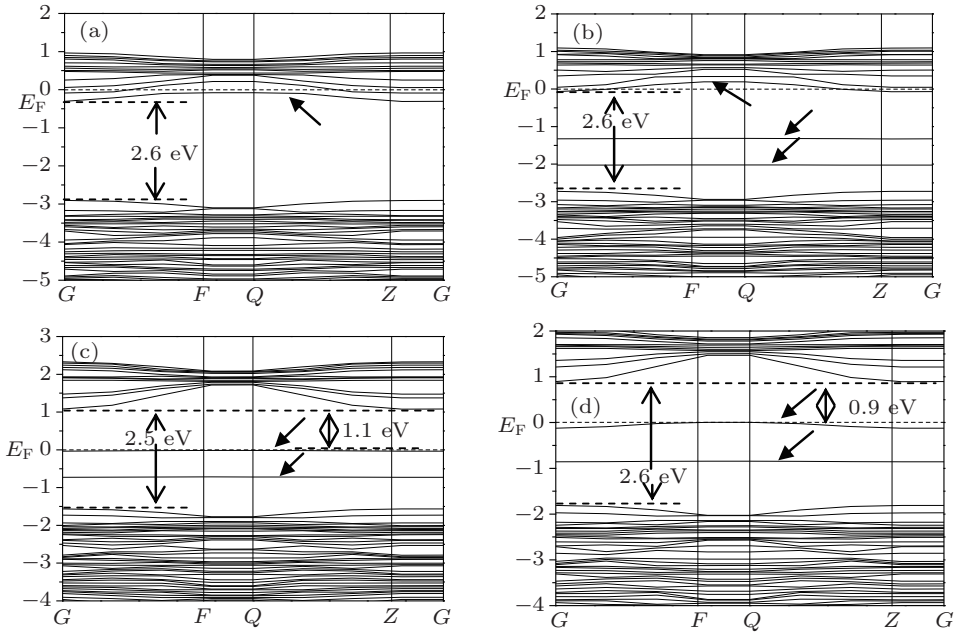


Fig. 4. Band structures of adsorption NO on the anatase TiO_2 (101) surface. (a) Surface with O vacancies, (b) NO horizontal adsorption, (c) N end adsorption, and (d) O end adsorption.

The surface electronic structure diagrams of the surfaces vertically adsorbed by the NO with N and O ends are shown in Figs. 4(c) and 4(d), respectively. A comparison among Figs. 4(c), 4(d), and 4(a) illustrates the absence of new bands at the bottom of the conduction band. An analysis of Fig. 3 shows that the N or O atom of NO is substantially adsorbed onto the surface vacancy site and fills the original O vacancy; thus, the new band produced by the O vacancy does not exist naturally. The band gap slightly changes, which is similar to the case of NO horizontal adsorption, and two new bands appear (down arrows). For the N end adsorption, the energy difference between the band which passes through the Fermi energy level and the bottom of the conduction band is 1.1 eV. For the O end absorption, the energy level passing through the Fermi energy band and the bottom of the conduction band has a gap width of 0.9 eV.

The densities of states of the surface before and after adsorption (Figs. 5–7) are calculated to determine the electronic contribution for the nearby Fermi level. The results show that the width of the valence band energy is approximately 6 eV. The valence band mainly consists of the O 2p orbital and a small amount of Ti 3d orbital hybridization. The width of the conduction band energy is approximately 1.5 eV and mainly consists of the Ti 3d orbital and a small part of the O 2p orbital. A band surface state is observed after adsorption.

In the N end adsorption, there are two surface states in the band gap. The total density of states (TDOS) and partial density of states (PDOS) [Figs. 5(a) and 5(b)] are calculated to investigate further the source of the surface state near the Fermi level. The surface states located at the Fermi level are mainly attributed to O 2p and N 2p orbital hybridizations, with contributions from the Ti 3d orbital. The surface state located below the Fermi level originates from the O 2p orbital, with contributions from Ti 3d and N 2p orbital hybridizations. The adsorption process is driven by atomic interactions. According to the analysis of the density of states, one can find that the Ti 3d and N 2p orbital hybridise together. In addition, the N and surface Ti atomic interactions are clearly very strong.

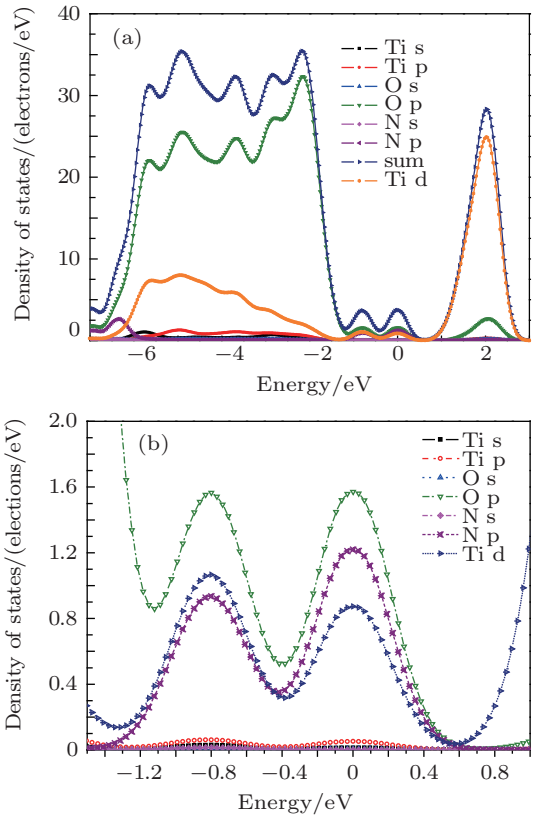


Fig. 5. (color online) Densities of states of anatase TiO_2 (101) surface adsorbing N terminal of NO molecule.

In the O end adsorption, the band gap also exists in two surface states. The TDOS and PDOS of the surface after adsorption are shown in Figs. 6(a) and 6(b), respectively. The surface states located at the Fermi level mainly come from the N 2p orbits, with contributions from the O 2p and Ti 3d orbits. The surface state under the Fermi level mainly consists of the orbital hybridizations of the N 2p, Ti 3d, and O 2p orbits. According to the analysis of the density of states and the Ti 3d and O 2p orbital hybridization, one can see that the interactions between the O atom and the superficial Ti atom are also very intense.

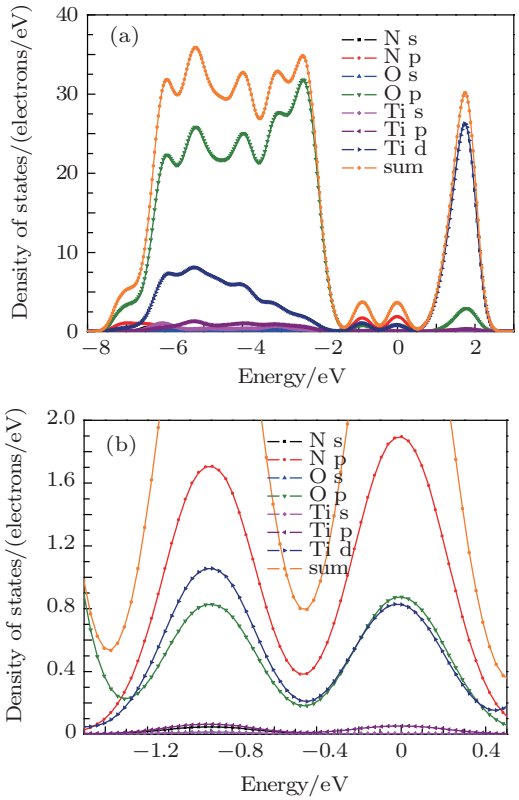


Fig. 6. (color online) Densities of states of anatase TiO_2 (101) surface adsorbing O end of NO molecule: (a) TDOS and (b) PDOS.

The NO horizontal adsorption and the surface state in the band gap virtually merge into one. The TDOS and PDOS are shown in Figs. 7(a) and 7(b), respectively. The surface states at the Fermi energy level mainly originates from the N 2p orbital, with secondary contributions from the O 2p and Ti 3d orbits. The N or O atom of the NO molecule has very intense interactions with the superficial Ti atom.

According to the angle analysis of density of states, one can understand that the N or O atom and the superficial Ti atom can have a very strong interaction. This interaction explains the ease of adsorption on the anatase TiO_2 (101) surface containing O vacancy defects. These findings are consistent with the results of the band structure analysis.

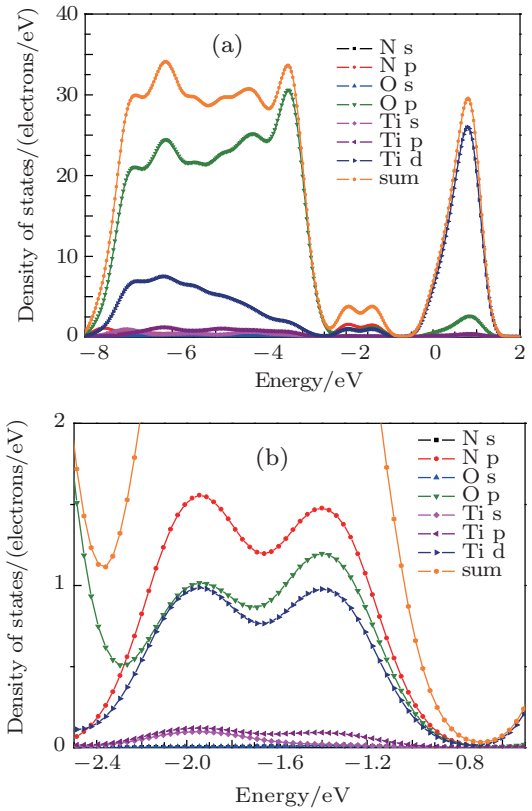


Fig. 7. (color online) Densities of states of anatase TiO_2 (101) surface horizontally adsorbing NO molecule.

3.5. Optical absorption spectrum

Figure 8 shows the optical absorption spectra of the NO molecules during adsorption onto the TiO_2 (101) surface containing O vacancies. A strong absorption peak is observed in the low-energy region of the TiO_2 (101) surface containing O vacancies, with a corresponding energy of approximately 0.9 eV. This result is consistent with those of the band structure diagram analysis, indicating that the presence of O vacancy defects on the TiO_2 (101) surface contributes to the absorption of visible light in the low-energy region. This conclusion is similar to the computed results presented by Hou *et al.*,[21] in which the bulk phase anatase TiO_2 with high oxygen-vacancy density significantly affects the red shift in the absorption spectrum. All these findings confirm that the surfaces with O vacancies facilitate the degradation of light. Figure 8 shows that the energy absorption peaks in the low-energy region have weakened to different degrees. The N and O end adsorptions are considerably weakened. The energy structure figure shows that the NO horizontal adsorption also has a clear absorption peak in the low-energy region. After NO adsorption, an absorption edge close to 2.6 eV is observed; this absorption edge has a small degree of red-shift compared with that before adsorption. When NO is adsorbed onto the TiO_2 (101) surface containing O vacancy defects, the main characteristics of the visible light absorption in the low-energy region show the weakening of the visible light to different degrees.

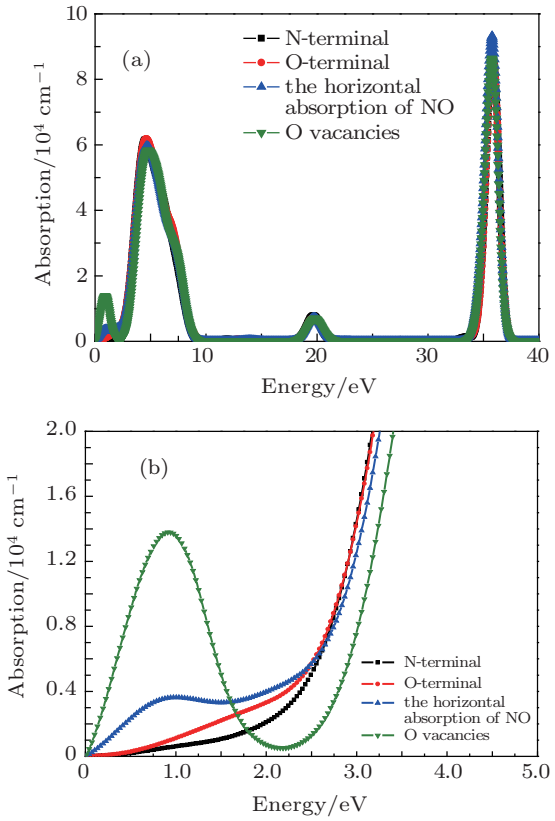


Fig. 8. (color online) Optical absorption spectra of TiO_2 (101) surface with O vacancies adsorbed NO molecule.

4. Conclusions

In this paper, the stable structure and electronic and optical properties of NO adsorption on the anatase TiO_2 (101) surface are studied using the first-principles density functional theory. The following results were obtained.

i) The NO molecules on the complete O_{2c} surface are not easily adsorbed, whereas the adsorption is easier on the anatase TiO_2 (101) surface containing O vacancy defects. Thus, a surface with a high concentration of O vacancies promotes NO adsorption.

ii) NO molecule adsorption on the anatase TiO_2 (101) surface containing O vacancies has a positive adsorption energy value and the adsorption process is exothermic, which results in a more stable adsorption structure.

iii) After horizontal adsorption, the charge transfer to the NO molecule weakens the N–O bond. The charge distribution behaviour also reveals that NO strongly interacts with the substrate surface.

iv) When the NO molecule is adsorbed onto the TiO_2 (101) surface containing O vacancies, the surface states located at the Fermi energy level mainly originate from the N 2p

orbits and the hybridization of a few O 2p orbits, with contributions from the Ti 3d orbits. The N and O atoms of NO and the substrate surface Ti atoms exhibit strong interactions.

v) The anatase TiO_2 (101) surface containing O vacancy defects contributes to the absorption of visible light in the low-energy region as well as to light degradation, whereas NO adsorption on the anatase TiO_2 (101) surface containing O vacancy defects weakens the effects of visible light absorption in the low-energy region.

References

[1] Wang Y 2005 *Acta Chim. Sin.* **63** 1023 (in Chinese)
[2] Wang Y and Meng L 2005 *Acta Phys. Sin.* **54** 2207 (in Chinese)
[3] Wang Y and Liu X 2006 *Journal of Lanzhou Jiaotong University (Natural Sciences)* **25** 47 (in Chinese)
[4] Ma X G, Tang C Q and Yang X H 2007 *J. Theor. Comput. Chem.* **6** 23
[5] Ma X G 2006 Ph. D. Dissertation, "The Theoretical Study of the Anatase TiO_2 Surface" (Wuhan: Huazhong University of Science and Technology) (in Chinese)
[6] Chen Q L, Tang C Q and Zheng G 2009 *Physica B: Conden. Matter* **404** 1074
[7] Chen Q L and Tang C Q 2009 *Acta Phys. Chim. Sin.* **25** 915
[8] Sun F Y and Shi H 2008 *Forest Engin.* **24** 48
[9] Sumita M, Hu C P and Tateyama Y 2010 *J. Phys. Chem. C* **114** 18529
[10] Finazzi E and Valentin C D 2007 *J. Phys. Chem. C* **111** 9275
[11] Long R, English N J and Dai Y 2009 *J. Phys. Chem. C* **113** 17464
[12] Wanbayor R, Deak P, Frauenheim T and Ruangpornvisuti V 2011 *J. Chem. Phys.* **134** 104701
[13] Wanbayor R and Ruangpornvisuti V 2010 *J. Mol. Structure: THEOCHEM* **925** 103
[14] Ma X G, Tang C Q, Huang J Q, Hu L F, Xue X and Zhou W B 2006 *Acta Phys. Sin.* **55** 4208 (in Chinese)
[15] Kresse G and Joubert D 1999 *Phys. Rev. B* **59** 1758
[16] Perdew J P, Ruzsinszky A, Csonka G I, Vydrov O A, Scuseria G E, Constantin L A, Zhou X and Burke K 2008 *Phys. Rev. Lett.* **100** 136406
[17] Yang Y, Feng Q, Wang W H and Wang Y 2013 *J. Semicond.* **34** 073004
[18] Hebenstreit W, Ruzycki N, Herman G S, Gao Y F and Diebold U 2000 *Phys. Rev. B* **62** 16334
[19] Ma X G, Jiang J J and Liang P 2008 *Acta Phys. Sin.* **57** 3120 (in Chinese)
[20] Han Y, Liu C J and Ge Q F 2006 *Phys. Chem. B* **110** 7463
[21] Hou Q Y, Zhang Y and Zhang T 2008 *Acta Phys. Sin.* **57** 1862 (in Chinese)